Published in final edited form as:
Cancer Res. 2014 November 1; 74(21): 6036–6047. doi:10.1158/0008-5472.CAN-14-1084.

Promoting Thiol Expression Increases The Durability of Antitumor T cell Functions

Pravin Kesarwani[#1], **Amir A. Al-Khami**[#1,§], **Gina Scurti**[2], **Krishnamurthy Thyagarajan**[1], **Navtej Kaur**[1], **Shahid Husain**[3], **Quan Fang**[1], **Osama S. Naga**[1], **Patricia Simms**[2], **Gyda Beeson**[4], **Christina Voelkel-Johnson**[5], **Elizabeth Garrett-Mayer**[6], **Craig C. Beeson**[4], **Michael I. Nishimura**[2], and **Shikhar Mehrotra**[1,*]

[1]Department of Surgery, Medical University of South Carolina, Charleston, SC 29425

[2]Department of Surgery, Loyola University, Maywood, IL 60153

[3]Department of Ophthalmology, Medical University of South Carolina, Charleston, SC 29425

[4]Department of Drug Discovery, Medical University of South Carolina, Charleston, SC 29425

[5]Department of Microbiology & Immunology, Medical University of South Carolina, Charleston, SC 29425

[6]Department of Biostatistics & Epidemiology, Medical University of South Carolina, Charleston, SC 29425

[#] These authors contributed equally to this work.

Abstract

Ex vivo-expanded $CD8^+$ T cells used for adoptive immunotherapy generally acquire an effector memory-like phenotype (T_{EM} cells). With regard to therapeutic applications, two undesired features of this phenotype *in vivo* are limited persistence and reduced anti-tumor efficacy, relative to $CD8^+$ T cells with a central memory-like phenotype (T_{CM} cells). Further, there is incomplete knowledge about all the differences between T_{EM} and T_{CM} cells that may influence tumor treatment outcomes. Given that T_{CM} cells survive relatively longer in oxidative tumor microenvironments, we investigated the hypothesis that T_{CM} possess relatively greater anti-oxidative capacity than T_{EM} cells. Here we report that T_{CM} cells exhibit a relative increase compared to T_{EM} cells in expression of cell surface thiols, a key target of cellular redox controls, along with other antioxidant molecules. Increased expression of redox regulators in T_{CM} cells inversely correlated with the generation of reactive oxygen and nitrogen species, proliferative capacity and glycolytic enzyme levels. Notably, TCR-transduced T cells pretreated with thiol donors, such as N-acetyl cysteine or rapamycin, up-regulated thiol levels and antioxidant genes. A comparison of anti-tumor $CD8^+$ T cell populations on the basis of surface thiol expression showed

[*] *Corresponding Author*: Shikhar Mehrotra, Ph.D. Department of Surgery Hollings Cancer Center (HO 512H) Medical University of South Carolina 86 Jonathan Lucas Street, Charleston, SC 29425, USA Phone: 843-792-9195; FAX: 843-792-2556; mehrotr@musc.edu.
[§]**Current address**: Stanley S. Scott Cancer Center, Louisiana State University Health Sciences Center, New Orleans, LA 70112.

Author contribution. PK, AAK designed and performed research, collected and analyzed data, and wrote the paper. PK, AAK, SH, KT, NK, QF, OSN, GB, CVJ performed research, collected and analyzed data. EGM, CCB, MIN designed research and analyzed the data. SM designed research, analyzed data, and wrote the paper.

that thiol-high cells persisted longer *in vivo* and exerted superior tumor control. Our results suggest that higher levels of reduced cell surface thiols are a key characteristic of T cells that can control tumor growth, and that profiling this biomarker may have benefits to T cell adoptive immunotherapy protocols.

Keywords

Human; CD62L; CTL; glutathione; thiols

INTRODUCTION

The clinical success of adoptive T cell immunotherapy of cancer has been linked to the persistence of effector T cells *in vivo* (1). Activation and expansion of antigen-specific T cells for adoptive immunotherapy requires prolonged stimulation of T cells, which results in a population with heterogeneous effector and/or memory phenotype (2). Although T cells with effector memory-like phenotype (T_{EM}) are the immediate effectors, it is believed that the ones with central memory-like phenotype (T_{CM}) are better in controlling tumor growth (3-5). Limited persistence and homing capability of T_{EM} cells is argued for its decreased potential to effectively control tumor growth (5). Therefore, reprogramming of T_{EM} cells towards T_{CM}-like cells, using different cytokines or forced expression of transcription factors, is being extensively investigated (6).

Recent studies have implicated a role for free sulfhydryl groups (-SH; also referred to as thiol) in the function of individual cell surface proteins (7, 8). The overall amount of thiols that define the antioxidant and reductive capacity of cells, differs among subsets of peripheral blood mononuclear cells (PBMCs) (7). These cell surface thiols (c-SH) can be manipulated *in vitro* by altering the levels of intracellular glutathione (iGSH; γ-glutamylcysteinylglycine), an ubiquitous intracellular thiol that maintains the cellular redox state and the integrity or function of proteins (9). The relationship between iGSH depletion and the generation of reactive oxygen species (ROS) that can accelerate apoptosis, has been recently addressed (10). In addition, ROS could also amplify phosphorylation of c-Jun (JNK) and Akt/mTOR pathways leading to decreased persistence of the activated T cell subsets (11). T cell activation also increases the cell metabolism and mitochondrial respiration rates (12). Recent reports have also shown that $CD8^+$ memory T cells, but not $CD8^+$ effector T cells, possess substantial mitochondrial spare respiratory capacity (SRC), and are a critical regulator of $CD8^+$ T cell memory development (13). Similarly, a key property of immediate effector T cells to secrete interferon-gamma (IFN-γ) is dependent on availability of glucose (14). While effector T cells express high surface levels of the glucose transporter Glut-1 and are highly glycolytic, regulatory T cells with high antioxidant capacity express low levels of Glut-1 and have high lipid oxidation rates (15). However, whether the differences in thiol/antioxidant capacity affect effector T cell persistence and its metabolic state impacting their functional outcome has not been addressed.

In this study, we compare the level of thiols/antioxidant along with metabolic commitment between the T_{CM} and T_{EM}-like cells and further evaluate if that contributes to differential

anti-tumor response. Our data suggests that manipulating the cellular redox state could be the key to prolonged survival of T cell populations that are otherwise sensitized to death, and improve adoptive immunotherapy protocols for the treatment of cancer.

METHODS

Cells, culture medium, and reagents

PBMCs from healthy donors were obtained from a commercial vendor, Research Blood Components, LLC (Brighton, MA), after institutional approval by the Human Investigation Review Board. Culture medium was Iscove's Modified Dulbecco's Medium (GIBCO BRL, Grand Island, NY) supplemented with 10% fetal bovine serum (Gemini Bioproducts, Inc., Calabasas, CA). Ficoll-Paque was obtained from Amersham Biosciences (Piscataway, NJ). Recombinant interleukin (IL)-15 and IL-2 were purchased from R & D Systems (Minneapolis, MN). Rapamycin was purchased from LC Laboratories (Woburn, MA). L-NAC was obtained from Sigma (St. Louis, MO). Fluorochrome-conjugated Annexin-V and monoclonal antibodies were obtained from BD Biosciences (San Jose, CA) or from BioLegend (San Diego, CA). CFSE was purchased from Molecular Probes (Carlsbad, CA).

Animals and cell lines

C57BL/6, Rag deficient mice ($Rag^{-/-}$), pMel and NSG ($NOD^{-/-}$, $SCID^{-/-}$, IL-2 receptor γ $chain^{-/-}$) mice were purchased from Jackson Laboratory, and stocks were maintained at MUSC animal facility in pathogen-free facilities and under the approved procedures of the Institutional Animal Care and Use Committee. T2 cells are transporter-associated protein-deficient and its empty surface HLA-A2 molecules were used for direct presentation of epitopes to the antigen-reactive CTL. B16-F10 ($H\text{-}2^{b}$) is a tyrosinase-positive murine melanoma.

iGSH and c-SH determination

For iGSH determination, cells were preloaded for 15 min with 10 μm monochlorobimane, which forms blue fluorescent adducts with iGSH (16, 17). Cell surface thiols were measured using Alexa Fluor 633-coupled maleimide (ALM-633; Invitrogen, Carlsbad, CA) (18). Cells were incubated with 5 μM ALM-633 for 20 min on ice.

Adoptive T cell Transfer

For adoptive transfer experiments naïve pMel cells were isolated from spleen. Cells were activated using hgp100 $peptide_{25\text{-}33}$ (KVPRNQDWL1 μg/mL) in presence of 50 IU/ml rhIL-2 for three days. Equal numbers of activated cells (1×10^{6} $CD8^{+}V\beta12^{+}$ were transferred in each mice (either $Rag^{-/-}$ or C57BL/6) bearing 7 days established B16-F10 tumors. rhIL-2 (20 μg/mouse/dose) was given twice daily intraperitoneally for 3 days starting immediately after adoptive transfer. When indicated cells were cultured in presence or absence of rapamycin (250 nM) or treated with LNAC (5mM). Sorting based on c-SH expression was done using 3 days activated cells stained for cSH and sorted based on cSH^{hi} or cSH^{lo} (after gating on $CD8^{+}V\beta12^{+}$ T cells). Tumors were measured twice every week. Human TCR transduced cell pre cultured for 3 days with rapamycin (250nM) or treated with L-NAC (5mM) was transfer in NSG mice.

Engineering of TCR-transduced human T cells

Tyrosinase-reactive TCR-transduced T cells (TIL1383i TCR^+) were generated as described earlier (19).

Flow cytometry and cell sorting

Samples were acquired on a FACSCalibur or LSR Fortessa flow cytometer (Becton Dickinson, Mountain View, CA), and data were analyzed using FlowJo software (Tree Star Inc., Ashland, OR). Cells were sorted either on FACS Aria II sorter (Becton Dickinson, Mountain View, CA) or MoFlo Astrios cell sorter (Beckman Coulter, Miami, FL). Detailed protocols for Activation induced T cell death (AICD), staining the cells for mitochondrial membrane potential (DiOC6), reactive oxygen species (ROS), reactive nitrogen species (RNS), iGSH, and glucose consumption assay (2NBDG), has been described in supplementary methods.

Measurement of mitochondrial oxygen consumption and glycolytic flux

Mitochondrial oxygen consumption rate (OCR) and glycolytic potential (ECAR, extra-cellular acidification rate) of the cells was measured using XF24 analyzer (Seahorse Bioscience, MA). Detailed procedure is provided in supplementary materials and methods.

Real-time PCR

Total RNA was isolated from pellets of the indicated T cell subsets ($2\text{-}5\times10^6$ cells/pellet) using Trizol reagent (Invitrogen). cDNA was generated from 1 μg total RNA using iScript cDNA Synthesis Kit (BioRad, Hercules, CA). Real time for individual genes was done using Sso advance SYBR green (Bio-rad Hercules, CA) and CFX96 Touch^{TM} real-time PCR detection system (BioRad). Primer sequences of the genes evaluated are provided in Supplementary Table 1.

Statistical methods

Comparisons across conditions were performed using paired *t* tests. When comparing fold-change and ratios, a log transform was applied before analysis. When comparing to a reference fold-change of 1 (or a ratio of 1), one-sample *t* tests were used where it was tested that the mean log fold-change (or log ratio) was equal to 0. Two-sample *t* tests were used to compare across conditions when no standardization was used, or standardization was performed within groups. When comparing mean florescence intensity (MFI) for flow cytometry data we used paired *t*-test. For comparing difference in number of cells between groups we utilized a log transformation and analyzed the data using paired *t*-test. To evaluate the difference between the c-SH^{lo} and c-SH^{hi} groups, a linear regression model was fit using generalized estimating equations (GEE) to account for repeated measures per mouse over time. To adhere to model assumptions, the outcome variable was square-root of tumor size and predictors were main effects of group (c-SH^{lo} vs. control; c-SH^{hi} vs. control), time (treated as continuous), interactions between group and time, and indicator variables of the experiment (to account for cohort effects). Robust standard errors were estimated and the correlation structure was assumed to be exchangeable. Tumor growth rate (i.e. slope) was compared across groups using Wald tests for the coefficients for the interactions between

group and time. Residual plots and graphical displays were used for model diagnostics. All tests are 2-sided and an alpha (or *p* value) of 0.05 was considered to be statistically significant.

RESULTS

Differential antioxidant capacity between T cell subsets regulates their sensitivity to cell death

Expansion of antigen-specific $CD8^+$ T cells *ex vivo* generates a population with heterogeneous effector and/or memory phenotype (2). Antigen-experienced T cell subsets can be identified phenotypically by a set of cell surface molecules: T_{CM} cells constitutively express $CD44^{hi}CD62L^{hi}$, whereas T_{EM} cells exhibit $CD44^{hi}CD62L^{lo}$ phenotype. We thus used CD44 and CD62L as markers to delineate the two T cell subsets and determine their sensitivity to apoptosis in our experiments. TCR restimulation of activated T cells resulted in relatively more death in $CD62L^{lo}$ $CD8^+$ and $CD4^+$ T cells as determined by increased distribution of Annexin-V (Fig. 1A). Similar results that correlate the $CD62L^{lo}$ population with higher extracellular translocation of Annexin-V and decreased mitochondrial membrane potential (a marker for apoptosis) were also observed, upon restimulation of activated PBMCs for 4 h with various stimuli (Fig. S1A-D). To confirm if the increased sensitivity of $CD62L^{lo}$ T cells to apoptosis was not a culture artifact, expression of anti-apoptotic protein BCL-XL was evaluated on CD62L T cell subsets sorted from human PBMCs of healthy donors. Our data shows that BCL-XL was substantially elevated in freshly sorted $CD62L^{hi}$, but not in $CD62L^{lo}$ $CD8^+$ T cell subsets (Fig. S1E). These data confirmed the innate differential sensitivity of the CD62L T cell subsets to activation-induced cell death.

Since ROS and RNS have previously been reported as potent innate effector molecules that also regulate activation-induced T cell apoptosis (11), we assessed the levels of these free radicals in $CD62L^{lo}$ and $CD62L^{hi}$ T cell subsets after 4 hours restimulation. Here, an increased generation of superoxide (DHE) and nitric oxide (DAF) in $CD62L^{lo}$ cells was observed, when compared to $CD62L^{hi}$ cells (Fig. S1F). Differences in key antioxidant proteins could contribute to the disparity of free radical accumulation and sensitivity to apoptosis between $CD62L^{lo}$ and $CD62L^{hi}$ T cells. Among them, iGSH plays a key role in regulating the intracellular redox balance and the status of cell surface thiol (c-SH) groups on other molecules (9). Using a cell surface marker-based comprehensive gating strategy to delineate T_{CM} cell ($CD8^+CD44^+CD62L^{hi}CXCR3^{lo}CCR7^+$) and T_{EM} ($CD8^+CD44^+CD62L^{lo}CXCR3^{hi}CCR7^-$) cells (Fig. S1G), our data showed that the $CD62L^{hi}$ T_{CM} cell had a higher expression of c-SH, as compared to $CD62L^{lo}$ T_{EM} subsets (Fig. 1Bi). In addition, the $CD62L^{hi}$ T cell subset had higher levels of iGSH over the $CD62L^{lo}$ T cell subset (Fig. 1Bii). An increased expression of the reductive –SH moiety and reduced iGSH allowed the $CD62L^{hi}$ T cell subset to withstand increased oxidative-stress induced by H_2O_2 (Fig. S2A). Our results also showed that an inverse correlation exists between T cell proliferation and cell surface thiol levels (Fig. 1C), i.e., a concomitant progressive reduction in CD62L expression and c-SH was observed in each daughter progeny of a proliferating T cell. The fluorescence intensity for CD62L expression and c-SH indicated that $CFSE^{hi}$ cells

that underwent less proliferation expressed increased cell surface thiol levels and CD62L, compared to CFSE^{lo} cells that underwent more proliferation (Figs. 1C and S2B). Further, expression of the thiol regulating thioredoxin proteins, TRX-1 and TRX-2, which act as antioxidants by facilitating the reduction of other proteins through cysteine thiol-disulfide exchange (20), was reduced in higher proliferating T cells (Fig. S2C). Moreover, the GSH/GSSG ratio (Fig. S2D) indicated the reduced glutathione was increased in sorted CD62L^{hi} T cells. Further, using real-time PCR arrays we also found an increased gene expression of the antioxidant molecules (Fig. S2E) in the FACS sorted CD62L^{hi} subset, compared to the CD62L^{lo} subset, that was confirmed with individual PCR (Fig. 1D). Altogether, these data indicate that CD62L^{hi} T cells are less susceptible to activation-induced apoptosis due to their significantly increased anti-oxidative capacity, as compared to CD62L^{lo} T cells.

Differential mitochondrial levels and glycolysis in CD62L T cell subsets

. Since CD62L^{lo} T cells have higher ROS and RNS (Fig. S1F), and mitochondria are the major source of these reactive species, we evaluated whether there exists a difference in total mitochondria levels between the T cell subsets. Our microscopy and FACS data revealed that CD62L^{lo} T cells have more mitochondrial mass than CD62L^{hi} T cells (Fig. 2Ai and 2Aii, respectively). While CD62L^{hi} T cells demonstrate a larger cytoplasm and dispersed mitochondrial distribution, CD62L^{lo} T cells had smaller cytoplasmic space with tightly-packed mitochondria (bright-field panels of Fig. 2Ai). Accordingly, a significantly higher ratio of mitochondrial DNA to nuclear DNA (mDNA/nDNA) was also observed in the CD62L^{lo} T cells suggesting a higher mitochondrial biogenesis rate (Fig. 2B). A higher number of active mitochondria would possibly explain the increased ROS accumulation in CD62L^{lo} T cells, as compared to CD62L^{hi} T cells (as observed in Figure S1F). Since the ability of effector T cells to secrete key cytokine has been shown to be dependent on utilizing glucose as carbon source (14, 21), we tested if the immediate effector ability of CD62L^{lo} T subsets correlates to their high glycolytic commitment. Our data show that CD62L^{lo} T cells expressed higher levels of glucose transporter Glut-1 (Fig. 2C), that correlates with increased glucose consumption as measured by the 2-NBDG uptake levels using flow cytometry (Fig. 2D). FACS sorted CD62L^{lo} T cells also exhibited an increased expression of the key glycolytic enzymes hexokinase II (HKII), pyruvate kinase M2 (PKM2), phosphofructokinase 2 (PFK2), pyruvate dehydrogenase kinase isozyme 1 (PDK1), and PDK2 as compared to CD62L^{hi} cells (Fig. 2E). The CD62L^{lo} T cells also exhibited higher expression of hypoxia inducible-factor 1 (HIF1α), relative to CD62L^{hi} cells. These observations establish that the mitochondrial distribution and the level of glycolytic molecules are different between the CD62L^{lo} T_{EM} and CD62L^{hi} T_{CM} subsets.

c-SH^{hi} T cell subsets are better at controlling tumor growth

We next evaluated if higher c-SH expressing T cells will have improved ability to control tumor growth. For this purpose, we first sorted the activated gp100 epitope-specific T cells based on c-SH expression and compared the expression of antioxidant and glycolytic molecules. A real-time expression analysis revealed that c-SH^{hi} cells have a lower expression of key glycolytic genes (HKII, HIF-1α, PFKII), but antioxidant (TRX1, SOD1) and effector molecules (as Granzyme B) were expressed at higher levels (Fig. 3A). In addition, the lower mitochondrial membrane potential, indicative of less active mitochondria

that correlates to reduced ROS accumulation, was also observed in c-SH^{hi} as compared to c-SH^{lo} cells (Fig. 3B). Adoptive transfer of c-SH^{hi} gp100 epitope-specific T cells resulted in improved and long lasting control of subcutaneously established B16 murine melanoma as compared to the group that received c-SH^{lo} T cells (Figs. 3C, and S2F for sorting strategy). The number of antigen specific T cells retrieved from c-SH^{hi} transferred group was higher (Fig. 3D, upper and lower left panels), and difference in c-SH expression between the groups was maintained at the experimental endpoint (Fig. 3E). Thus, our data supports that thiol expression is directly proportional to T cell persistence and tumor control.

Rapamycin treatment enhances c-SH levels in T cells

The data presented thus far supported that the c-SH expression correlated with the T_{CM} phenotype, increased antioxidant capacity, and reduced glycolysis. While identifying potent long-term persisting anti-tumor T cells based on expression c-SH expression could be a potential therapeutic strategy, we wanted to test if using pharmacological agents can render higher thiols/antioxidant capacity to *ex vivo* expanded human T cells (with primarily T_{EM} phenotype). Since rapamycin treatment has been shown to induce a higher expression of CD62L on CD8$^+$ T cells *in vitro* and *in vivo* (22), we tested if treating the human T cells with rapamycin also induced c-SH and affects metabolic pathways. Consistent with previous studies (23), culturing human PBMCs with rapamycin for five days resulted in a higher expression of CD62L (Fig. S3A). Interestingly, rapamycin treatment also increased the levels of cell surface thiols (c-SH) on CD8$^+$ T cells (Fig. S3B, upper panel). In accordance with the previous study that showed an inverse correlation with c-SH and ROS (18), rapamycin-treated cells with increased c-SH have lesser accumulation of superoxide as compared to control T cells after restimulation, as measured by DHE staining (Fig. S3B, lower panel). Furthermore, as compared to untreated control cells, rapamycin-induced c-SH provided an optimal reductive environment to withstand the H_2O_2-induced oxidant injury and rescued both CD62L^{lo} and CD62L^{hi} subsets from H_2O_2-induced apoptosis (Fig. S3C). These data suggested that rapamycin could act by altering the expression of genes involved in oxidative stress and thereby, apoptosis. Indeed, we found that rapamycin upregulated the expression of antioxidant genes such as catalase, NRF-2, SOD-1, and TRX-2 (Fig. S3D). Further, a real time PCR array analysis of 84 genes related to oxidative stress ROS metabolism showed an increased expression of 15 anti-oxidative genes in rapamycin-treated T cells over untreated control (Table 1). These data suggested that upregulation of the T cell antioxidant response could be one of the mechanisms by which rapamycin affects memory CD8$^+$ T cell differentiation.

Since we observed that rapamycin, the mTOR-specific inhibitor, induces an increase in thiol levels that correlated with its ability to upregulate CD62L expression, we next investigated if the opposite is true; that is, whether an increased thiol expression affects the mTOR pathway. Because cellular availability of cysteine is considered to be a rate-limiting factor in the synthesis of thiol iGSH, we used the simplest cysteine derivative, L-NAC, a thiol antioxidant and iGSH precursor (24), to artificially increase the levels of reduced thiols on T cells. As observed in Figure S3E, upon L-NAC pretreatment, an elevation in the cell surface thiol levels was observed. In addition, we also observed that L-NAC pretreated T cells showed a downregulation of the pS6, a downstream molecule in the mTOR pathway, upon

TCR restimulation (Fig. S3F). To further determine the effect of increased thiol expression in a transnationally relevant model, we used the melanoma-associated human tyrosinase TCR TIL1383I-transduced T cells. Pretreatment of TCR-transduced T cells with L-NAC and rapamycin increased the expression of both cell surface thiols and iGSH (Fig. 4A). Further, antigen-specific restimulation of the TCR-transduced T cells pretreated with L-NAC and rapamycin also showed a reduction in TCR-restimulated induced cell death (Fig. 4B).

c-SH expression inversely correlates to T cell mitochondrial metabolism

Since rapamycin treatment of T cells increased the c-SH expression that correlated to increased antioxidant molecules and lower intracellular ROS, we next investigated if thiol donor L-NAC or rapamycin affected mitochondrial function. Mitochondrial metabolism has been shown to affect the generation of memory T cells after *ex vivo* culture in the presence of IL-15 (a cytokine that also induces $CD62L^{hi}$ phenotype) (25). We used the Seahorse Bioscience analyzer to measure mitochondrial function in real time using multi-well plates. Using carbonyl cyanide *p*-tri-fluoro-methoxy-phenylhydrazone (FCCP)-uncoupled respiration as a marker of maximal electron transport chain activity, we first confirmed that uncoupled oxygen consumption rate (OCR), an indicator of oxidative phosphorylation (OXPHOS), was higher in cells expanded in the presence of IL-15 as opposed to IL-2 (Fig. S3G) (13). However, pretreatment of IL-15-cultured T cells with rapamycin and L-NAC resulted in lower basal and uncoupled OCR (Fig. 4Ci). A similar decrease in basal and maximal OCR was observed when TIL1383I TCR-transduced T cells were pretreated with rapamycin and L-NAC (Fig. 4Cii). The decrease in OCR by rapamycin and L-NAC pretreatment was also reflected by the decreased expression of the mitochondria-specific 12S ribosomal RNA, cytochrome *b* (a component of respiratory chain complex III), cytochrome *c* oxidase subunit 2 (COXII), and NADH dehydrogenase 4 (ND4) (Fig. 4D). In addition, mitochondrial transcription factor A (TFAM) along with the key mitochondrial biogenesis regulator peroxisome proliferator-activated receptor gamma coactivator 1-alpha (PGC-1α) (Fig. 4D) was also found to be down-regulated after the pretreatment of T cells with rapamycin and L-NAC. The rapamycin and L-NAC-mediated decrease of mitochondrial biogenesis in T cells could be considered as a quality-control process that decreases the dysfunctional mitochondria under conditions of cell intrinsic oxidative stress due to reduced antioxidant levels (26). Further, the decrease in mitochondrial content of the T cells after pretreatment with rapamycin and L-NAC was confirmed by microscopy (Fig. 4E). These data confirmed that thiol upregulation (mediated herein by rapamycin and L-NAC) significantly reduced mitochondrial biogenesis and mitochondrial respiratory capacity.

c-SH expression inversely correlates to T cell glycolysis

Since rapamycin and LNAC pretreatment increased c-SH expression, but decreased the mitochondrial function, we next evaluated if these agents also affected the glycolytic pathway (12). Our data showed that rapamycin and L-NAC-pretreated TIL1383I TCR-transduced cells exhibited a decrease in glucose consumption as measured by 2NBDG analysis for glucose uptake (Fig. 5Ai and 5Aii). Further, evaluation of glycolysis in real-time, using the Seahorse analyzer, also showed a decrease in the extracellular acidification

rate (ECAR) of TIL1383I TCR-transduced T cells in the presence of rapamycin and L-NAC (Fig. 5B). Western blot analyses also confirmed for the lower HIF-1α expression that correlates with decreased glycolysis in the presence of rapamycin in TCR-transduced T cells (Fig. 5C). These results are different than those reported in other model systems where rapamycin induces glycolysis (27), raising the possibility that hyperactive T cells may be more sensitive to inhibition of mTOR or glycolysis.

To explore the *in vivo* persistence of TCR-transduced T cells that have an increased thiol expression/antioxidant capacity and lowered glycolysis after pretreatment with rapamycin or L-NAC, cells were adoptively-transferred into NSG mice (NOD *scid* IL-2 receptor gamma chain knockout mice), and these homeostatically-maintained cells were retrieved after two days. Our data showed that 2- to 3-fold more cells were retrieved from the rapamycin or L-NAC pretreated groups as compared to the controls (Fig. 5Di), and the retrieved cells retained a much higher CD62L expression after *in vivo* transfer (5Dii). To confirm if the increased number of T cells along with the expression of CD62L resulted in an improvement in the anti-tumor T cell response, gp100 melanoma epitope-reactive T cells (untreated or pre-treated with rapamycin) were adoptively-transferred to C57BL/6 $Rag^{-/-}$ mice with subcutaneously established B16 murine melanoma. Rapamycin was also administered intraperitoneally every alternate day for two weeks, as reported earlier (28). In agreement with this study (28), our data also showed that the mice receiving rapamycin-treated T cells had improved tumor control (Fig. 5Ei). The improvement could be attributed to the increased persistence of the transferred effectors with a $CD62L^{hi}$ phenotype (Fig. 5Eii). Importantly, an analysis of the retrieved-effector T cells from the tumor-bearing recipient mouse showed that rapamycin-treated T cells had better persistence (Fig. 5Eiii), which also correlated to higher c-SH^{hi} expression as compared to the untreated cells (Fig. 5Eiv). These data suggest that the strategy to increase c-SH expression (or antioxidant property) may centrally regulate effector T cell persistence, that in turn results in improved tumor control.

DISCUSSION

Adoptive cell therapy requires activation and expansion of tumor epitope-specific T cells *ex vivo*. However, rapid expansion to obtain high number of cells needed for transfer also confers a major fraction of these effectors with a replicative senescence phenotype resulting in impaired *in vivo* persistence (3, 29, 30). While strategies to minimally expand the effector T cells and conserve the T_{CM} and stemness phenotype are underway, we focused on deciphering the innate differences between the T cell subsets obtained after activation/expansion. We demonstrate here that T_{CM}-like cells have higher thiols/antioxidant levels, and less glucose requirement, as compared to T_{EM}-like cells. Importantly, a comparison of anti-tumor potential of the T cells, when sorted based on thiol expression, showed better persistence and tumor control *in vivo* by high thiol-expressing T cells. Our data indicated that both extracellular (≈ c-SH) and intracellular (≈ glutathione) distribution of antioxidant proteins in $CD8^+$ T cell subsets correlated with their decreased metabolic state and enhanced persistence of effector T cells.

To evaluate the contribution of redox molecules in T cell persistence, we used CD62L and CD44 expression for delineating between the two key subsets (i.e., T_{EM}-like and T_{CM}-like).

Our data established an inverse correlation between CD62L expression and ROS accumulation, which has been previously implicated by us in T cell death (11). Each cycle of repetitive TCR stimulation of epitope-specific T cells was recently shown to cause loss of CD62L expression in approximately 20% of the cells *in vivo* (i.e., 20% of $CD62L^{hi}$ cells convert to $CD62L^{lo}$ during each division *in vivo*) (31). Whereas compromised T cell homing ability due to loss of CD62L expression has been identified as one factor for the reduced *in vivo* efficacy of $CD62L^{lo}$ versus $CD62L^{hi}$ T cells (4, 5), our data suggested that the concomitant loss of c-SH (along with CD62L) in $CD8^+$ effector T cells accompanying proliferation could also play a major role in persistence. Both c-SH and iGSH play a role in modulating redox-regulated signal transduction and apoptosis, as iGSH depletion was shown to be necessary for the progression of apoptosis activated by both extrinsic and intrinsic signaling pathways (10). In addition, our data show that thioredoxins, proteins that act as antioxidants by facilitating the reduction of other proteins by cysteine thiol-disulfide exchange (20), were also reduced in T cells that underwent proliferation upon repeated TCR stimulation.

A recent study showed that a lower ROS-producing capacity is associated with an increased number of reduced cellular thiol groups (c-SH) on T cell membranes, that determines its reactivity and arthritis susceptibility (18, 32). The difference in c-SH in T cell subsets with distinct phenotype and susceptibility to death suggests that cell fate is directly linked to modulation of redox regulating proteins, and that in turn could affect ROS/RNS balance resulting in modulation of TCR dependent and independent signaling molecules/pathways (33-35). The inverse correlation between L-NAC induced c-SH expression and phosphorylation of S6 (a downstream molecule in the mTOR pathway) supports this view. Importantly, rapamycin treatment not only blocked mTOR activation, but also increased c-SH expression and the antioxidant level in T cells. Whereas up-regulated mTOR activity is associated with higher levels of intracellular ROS (36), lowering mTOR activation and concomitantly increasing c-SH/antioxidant levels is important for decreasing the susceptibility of oxidative stress-induced cell death. Thus, our work identifies a role for c-SH in suppressing mTOR signaling that is also known to affect mitochondrial function (36). Our data also showed that both rapamycin and L-NAC pretreated T cells with high c-SH had a low basal oxygen consumption rate compared to untreated cells, but they did not show a high spare respiratory capacity. Although rapamycin has been shown to promote the $CD62L^{hi}$ phenotype (as does IL-15), our data suggested that rapamycin and L-NAC pre-treatment resulted in decreased mitochondrial biogenesis and reduced expression of key glycolytic molecules in $CD62L^{hi}$ T_{CM}-like cells. It is evident that $CD62L^{hi}$ T cells generated under different conditions of cytokines (as IL-15) or after modulation of different pathways (using rapamycin), may be phenotypically similar, but metabolically dissimilar (37, 38). While earlier reports have addressed the role of metabolism in T cell activation and differentiation (12, 39, 40), its role in T cell contraction and regulating anti-tumor response is beginning to be addressed (13, 41). A recent publication showing pretreatment of CTL with the glycolytic inhibitor, 2-DG, results in improvement of the anti-tumor response, also supports our data (42). Another study also shows that T cells have the ability to interchangeably adapt to OXPHOS or glycolysis, and both metabolic pathways may exist in tandem to meet the energy needs of a T cell (43). While this study did not address if the

heterogeneous effector T cell population had a similar degree of metabolic commitment to one pathway or the other, our data showed that CD62L^{lo} T_{EM}-like cells have both higher glycolysis and OXPHOS than CD62L^{hi} T_{CM}-like cells, and that rapamycin treatment reduced the metabolically-active state and increased the antioxidant capacity that enables increased persistence in the tumor microenvironment. Further, if the differential accumulation of ROS in c-SH^{hi} *vs.* c-SH^{lo} T cell subset results in autophagy (involving Atg4, catalase, and the mitochondrial electron transport chain) mediated difference in cell survival *vs.* cell death respectively needs to be investigated (44).

Under normal conditions, intracellular redox status is reductive. Reduced thiols have also been shown to be important for antigen presentation and redox remodeling of antigen specific T cells (45, 46). It is likely that the thiol transfer from the mature DCs renders a subset of T cells with more thiols resulting in their improved fitness, and ability to overcome oxidative stress (47). Earlier studies have also shown that Treg's that have the ability to survive better than the effector T cells could be due to high level of reduced thiols expressed on their surface (15). Importantly, Treg's have also been shown to interfere with the glutathione metabolism in DCs resulting in ineffective antigen presentation and enforcing suppression (48). Additionally, the myeloid derived suppressor cells (MDSCs) have also been shown to mediate T cell suppression by depriving them of the cysteine that is require for T activation and function (49). Thus, the maintenance of the redox molecules as thiols may play an important role not only in boosting antigen presentation, but also overcoming immunosuppression and increasing survival of T cells. Our data suggested that on TCR restimulation there was a decrease in the reductive state of actively dividing cells (identified here as CD62L^{lo}T_{EM}-like cells), rendering them more sensitive to oxidative stress. Since protein-thiols are usually the sites of oxidation/nitrosylation, increased incidence of protein glutathionylation in CD62L^{hi} T_{CM}-like cells (induced by IL-15 or rapamycin) can protect protein-thiols from irreversible oxidation and/or prevent protein misfolding through disulfide formation, thus resulting in enhanced persistence. Importantly, the T cells with high c-SH/antioxidant expression also co-exhibit key anti-tumor properties as low glycolysis, increased persistence and controlled tumor growth. This suggested that thiol expression could serve as a biomarker that tightly correlates to better survival and anti-tumor T cell function, specifically in the presence of ROS and RNS-producing cells in the tumor microenvironment, inflammatory sites, or in the periphery of tumor patients. Therefore, as depicted in Fig. S4, we conclude that promoting the reductive cellular environment could affect metabolic function and result in the long-term maintenance of CD8^{+} T cells, with implications for adoptive immunotherapy approaches.

Supplementary Material

Refer to Web version on PubMed Central for supplementary material.

Acknowledgments

Authors acknowledge help from Drs. Xue-Zhong Yu, Chenthamarkshan Vasu, Chrystal Paulos at MUSC, and Dr. Jose-Alesandro Guevara at Loyola Medical Centre, Chicago for critical reading of this manuscript and their valuable feedback. Authors also thank Drs. Luanna Bartholomew and Radhika Gudi for their help in preparing this manuscript.

The work was supported in part by NIH grants R21CA137725 and R01CA138930, R01AR057643 (S.M.); R01CA104947 and P20GM10354202 (C.C.B.); and P01CA154778 (M.I.N.).

Abbreviations

ALM-633	Alexa Fluor 633-coupled maleimide
CTLs	cytotoxic T lymphocytes
DAF	4-amino-5-methylamino-2’,7’-difluoroflourescein diacetate
$DiOC_6$	dihexyloxacarbocyanine iodide
DHE	dihydroethydium
ECAR	Extra cellular acidification rate
FCCP	Carbonyl cyanide 4-(trifluoromethoxy)phenylhydrazone
HK	Hexokinase
L-NAC	N-acetyl-L-cysteine
NRF	Nuclear respiratory factor
OCR	Oxygen Consumption Rate
PBLs	peripheral blood leucocytes
PBMCs	peripheral blood mononuclear cells
PCD	programmed cell death
PDK	Pyruvate Dehydrogenase Kinase
PFK	Phosphofructokinase
PHA	Phytohaemagglutinin
RNS	reactive nitrogen species
ROS	reactive oxygen species
SOD	Super Oxide Dismutase
Treg	regulatory T cells
T_{CM}	central memory
T_{EM}	effector memory
TNF-α	tumor necrosis factor α
TRX	Thioredoxin

REFERENCES

1. Shen X, Zhou J, Hathcock KS, Robbins P, Powell DJ Jr. Rosenberg SA, et al. Persistence of tumor infiltrating lymphocytes in adoptive immunotherapy correlates with telomere length. J Immunother. 2007; 30:123–9. [PubMed: 17198091]
2. Hinrichs CS, Gattinoni L, Restifo NP. Programming CD8+ T cells for effective immunotherapy. Current opinion in immunology. 2006; 18:363–70. [PubMed: 16616471]

3. Gattinoni L, Klebanoff CA, Palmer DC, Wrzesinski C, Kerstann K, Yu Z, et al. Acquisition of full effector function in vitro paradoxically impairs the in vivo antitumor efficacy of adoptively transferred CD8+ T cells. The Journal of clinical investigation. 2005; 115:1616–26. [PubMed: 15931392]

4. Klebanoff CA, Gattinoni L, Torabi-Parizi P, Kerstann K, Cardones AR, Finkelstein SE, et al. Central memory self/tumor-reactive CD8+ T cells confer superior antitumor immunity compared with effector memory T cells. Proceedings of the National Academy of Sciences of the United States of America. 2005; 102:9571–6. [PubMed: 15980149]

5. Berger C, Jensen MC, Lansdorp PM, Gough M, Elliott C, Riddell SR. Adoptive transfer of effector CD8+ T cells derived from central memory cells establishes persistent T cell memory in primates. The Journal of clinical investigation. 2008; 118:294–305. [PubMed: 18060041]

6. Jameson SC, Masopust D. Diversity in T cell memory: an embarrassment of riches. Immunity. 2009; 31:859–71. [PubMed: 20064446]

7. Sahaf B, Heydari K, Herzenberg LA. Lymphocyte surface thiol levels. Proceedings of the National Academy of Sciences of the United States of America. 2003; 100:4001–5. [PubMed: 12642656]

8. Pedersen-Lane JH, Zurier RB, Lawrence DA. Analysis of the thiol status of peripheral blood leukocytes in rheumatoid arthritis patients. Journal of leukocyte biology. 2007; 81:934–41. [PubMed: 17210617]

9. Meister A, Anderson ME. Glutathione. Annu Rev Biochem. 1983; 52:711–60. [PubMed: 6137189]

10. Franco R, Cidlowski JA. Apoptosis and glutathione: beyond an antioxidant. Cell death and differentiation. 2009; 16:1303–14. [PubMed: 19662025]

11. Norell H, Martins da Palma T, Lesher A, Kaur N, Mehrotra M, Naga OS, et al. Inhibition of superoxide generation upon T-cell receptor engagement rescues Mart-1(27-35)-reactive T cells from activation-induced cell death. Cancer research. 2009; 69:6282–9. [PubMed: 19638595]

12. Michalek RD, Rathmell JC. The metabolic life and times of a T-cell. Immunological reviews. 2010; 236:190–202. [PubMed: 20636818]

13. van der Windt GJ, Everts B, Chang CH, Curtis JD, Freitas TC, Amiel E, et al. Mitochondrial respiratory capacity is a critical regulator of CD8+ T cell memory development. Immunity. 2012; 36:68–78. [PubMed: 22206904]

14. Cham CM, Gajewski TF. Glucose availability regulates IFN-gamma production and p70S6 kinase activation in CD8+ effector T cells. Journal of immunology. 2005; 174:4670–7.

15. Mougiakakos D, Johansson CC, Kiessling R. Naturally occurring regulatory T cells show reduced sensitivity toward oxidative stress-induced cell death. Blood. 2009; 113:3542–5. [PubMed: 19050306]

16. Franco R, Panayiotidis MI, Cidlowski JA. Glutathione depletion is necessary for apoptosis in lymphoid cells independent of reactive oxygen species formation. J Biol Chem. 2007; 282:30452–65. [PubMed: 17724027]

17. Sebastia J, Cristofol R, Martin M, Rodriguez-Farre E, Sanfeliu C. Evaluation of fluorescent dyes for measuring intracellular glutathione content in primary cultures of human neurons and neuroblastoma SH-SY5Y. Cytometry A. 2003; 51:16–25. [PubMed: 12500301]

18. Gelderman KA, Hultqvist M, Holmberg J, Olofsson P, Holmdahl R. T cell surface redox levels determine T cell reactivity and arthritis susceptibility. Proceedings of the National Academy of Sciences of the United States of America. 2006; 103:12831–6. [PubMed: 16908843]

19. Nishimura MI, Avichezer D, Custer MC, Lee CS, Chen C, Parkhurst MR, et al. MHC class I-restricted recognition of a melanoma antigen by a human CD4+ tumor infiltrating lymphocyte. Cancer research. 1999; 59:6230–8. [PubMed: 10626817]

20. Patenaude A, Ven Murthy MR, Mirault ME. Mitochondrial thioredoxin system: effects of TrxR2 overexpression on redox balance, cell growth, and apoptosis. The Journal of biological chemistry. 2004; 279:27302–14. [PubMed: 15082714]

21. Chang CH, Curtis JD, Maggi LB Jr. Faubert B, Villarino AV, O'Sullivan D, et al. Posttranscriptional control of T cell effector function by aerobic glycolysis. Cell. 2013; 153:1239–51. [PubMed: 23746840]

22. Araki K, Turner AP, Shaffer VO, Gangappa S, Keller SA, Bachmann MF, et al. mTOR regulates memory CD8 T-cell differentiation. Nature. 2009; 460:108–12. [PubMed: 19543266]

23. Araki K, Ellebedy AH, Ahmed R. TOR in the immune system. Current opinion in cell biology. 2011; 23:707–15. [PubMed: 21925855]
24. Droge W, Kinscherf R, Mihm S, Galter D, Roth S, Gmunder H, et al. Thiols and the immune system: effect of N-acetylcysteine on T cell system in human subjects. Methods Enzymol. 1995; 251:255–70. [PubMed: 7651204]
25. Klebanoff CA, Finkelstein SE, Surman DR, Lichtman MK, Gattinoni L, Theoret MR, et al. IL-15 enhances the in vivo antitumor activity of tumor-reactive CD8+ T cells. Proceedings of the National Academy of Sciences of the United States of America. 2004; 101:1969–74. [PubMed: 14762166]
26. Yoboue ED, Devin A. Reactive oxygen species-mediated control of mitochondrial biogenesis. International journal of cell biology. 2012; 2012:403870. [PubMed: 22693510]
27. Sun Q, Chen X, Ma J, Peng H, Wang F, Zha X, et al. Mammalian target of rapamycin up-regulation of pyruvate kinase isoenzyme type M2 is critical for aerobic glycolysis and tumor growth. Proceedings of the National Academy of Sciences of the United States of America. 2011; 108:4129–34. [PubMed: 21325052]
28. Li Q, Rao R, Vazzana J, Goedegebuure P, Odunsi K, Gillanders W, et al. Regulating mammalian target of rapamycin to tune vaccination-induced CD8(+) T cell responses for tumor immunity. J Immunol. 2012; 188:3080–7. [PubMed: 22379028]
29. Tran KQ, Zhou J, Durflinger KH, Langhan MM, Shelton TE, Wunderlich JR, et al. Minimally cultured tumor-infiltrating lymphocytes display optimal characteristics for adoptive cell therapy. J Immunother. 2008; 31:742–51. [PubMed: 18779745]
30. Zhou J, Shen X, Huang J, Hodes RJ, Rosenberg SA, Robbins PF. Telomere length of transferred lymphocytes correlates with in vivo persistence and tumor regression in melanoma patients receiving cell transfer therapy. J Immunol. 2005; 175:7046–52. [PubMed: 16272366]
31. Schlub TE, Badovinac VP, Sabel JT, Harty JT, Davenport MP. Predicting CD62L expression during the CD8+ T-cell response in vivo. Immunology and cell biology. 88:157–64. [PubMed: 19859082]
32. Hultqvist M, Backlund J, Bauer K, Gelderman KA, Holmdahl R. Lack of reactive oxygen species breaks T cell tolerance to collagen type II and allows development of arthritis in mice. Journal of immunology. 2007; 179:1431–7.
33. Ibiza S, Victor VM, Bosca I, Ortega A, Urzainqui A, O'Connor JE, et al. Endothelial nitric oxide synthase regulates T cell receptor signaling at the immunological synapse. Immunity. 2006; 24:753–65. [PubMed: 16782031]
34. Snyder CM, Shroff EH, Liu J, Chandel NS. Nitric oxide induces cell death by regulating anti-apoptotic BCL-2 family members. PloS one. 2009; 4:e7059. [PubMed: 19768117]
35. Vig M, Srivastava S, Kandpal U, Sade H, Lewis V, Sarin A, et al. Inducible nitric oxide synthase in T cells regulates T cell death and immune memory. The Journal of clinical investigation. 2004; 113:1734–42. [PubMed: 15199408]
36. Ramanathan A, Schreiber SL. Direct control of mitochondrial function by mTOR. Proceedings of the National Academy of Sciences of the United States of America. 2009; 106:22229–32. [PubMed: 20080789]
37. Chen C, Liu Y, Liu R, Ikenoue T, Guan KL, Zheng P. TSC-mTOR maintains quiescence and function of hematopoietic stem cells by repressing mitochondrial biogenesis and reactive oxygen species. The Journal of experimental medicine. 2008; 205:2397–408. [PubMed: 18809716]
38. Li Q, Rao RR, Araki K, Pollizzi K, Odunsi K, Powell JD, et al. A central role for mTOR kinase in homeostatic proliferation induced CD8+ T cell memory and tumor immunity. Immunity. 2011; 34:541–53. [PubMed: 21511183]
39. Jones RG, Thompson CB. Revving the engine: signal transduction fuels T cell activation. Immunity. 2007; 27:173–8. [PubMed: 17723208]
40. Pearce EL, Poffenberger MC, Chang CH, Jones RG. Fueling immunity: insights into metabolism and lymphocyte function. Science. 2013; 342:1242454. [PubMed: 24115444]
41. Sena LA, Li S, Jairaman A, Prakriya M, Ezponda T, Hildeman DA, et al. Mitochondria are required for antigen-specific T cell activation through reactive oxygen species signaling. Immunity. 2013; 38:225–36. [PubMed: 23415911]

42. Beneteau M, Zunino B, Jacquin MA, Meynet O, Chiche J, Pradelli LA, et al. Combination of glycolysis inhibition with chemotherapy results in an antitumor immune response. Proceedings of the National Academy of Sciences of the United States of America. 2012; 109:20071–6. [PubMed: 23169636]
43. Sukumar M, Liu J, Ji Y, Subramanian M, Crompton JG, Yu Z, et al. Inhibiting glycolytic metabolism enhances CD8+ T cell memory and antitumor function. The Journal of clinical investigation. 2013; 123:4479–88. [PubMed: 24091329]
44. Gibson SB. Investigating the role of reactive oxygen species in regulating autophagy. Methods in enzymology. 2013; 528:217–35. [PubMed: 23849868]
45. Angelini G, Gardella S, Ardy M, Ciriolo MR, Filomeni G, Di Trapani G, et al. Antigen-presenting dendritic cells provide the reducing extracellular microenvironment required for T lymphocyte activation. Proceedings of the National Academy of Sciences of the United States of America. 2002; 99:1491–6. [PubMed: 11792859]
46. Martner A, Aurelius J, Rydstrom A, Hellstrand K, Thoren FB. Redox remodeling by dendritic cells protects antigen-specific T cells against oxidative stress. Journal of immunology. 2011; 187:6243–8.
47. Thoren FB, Betten A, Romero AI, Hellstrand K. Cutting edge: Antioxidative properties of myeloid dendritic cells: protection of T cells and NK cells from oxygen radical-induced inactivation and apoptosis. Journal of immunology. 2007; 179:21–5.
48. Yan Z, Garg SK, Banerjee R. Regulatory T cells interfere with glutathione metabolism in dendritic cells and T cells. The Journal of biological chemistry. 2010; 285:41525–32. [PubMed: 21037289]
49. Srivastava MK, Sinha P, Clements VK, Rodriguez P, Ostrand-Rosenberg S. Myeloid-derived suppressor cells inhibit T-cell activation by depleting cystine and cysteine. Cancer research. 2010; 70:68–77. [PubMed: 20028852]

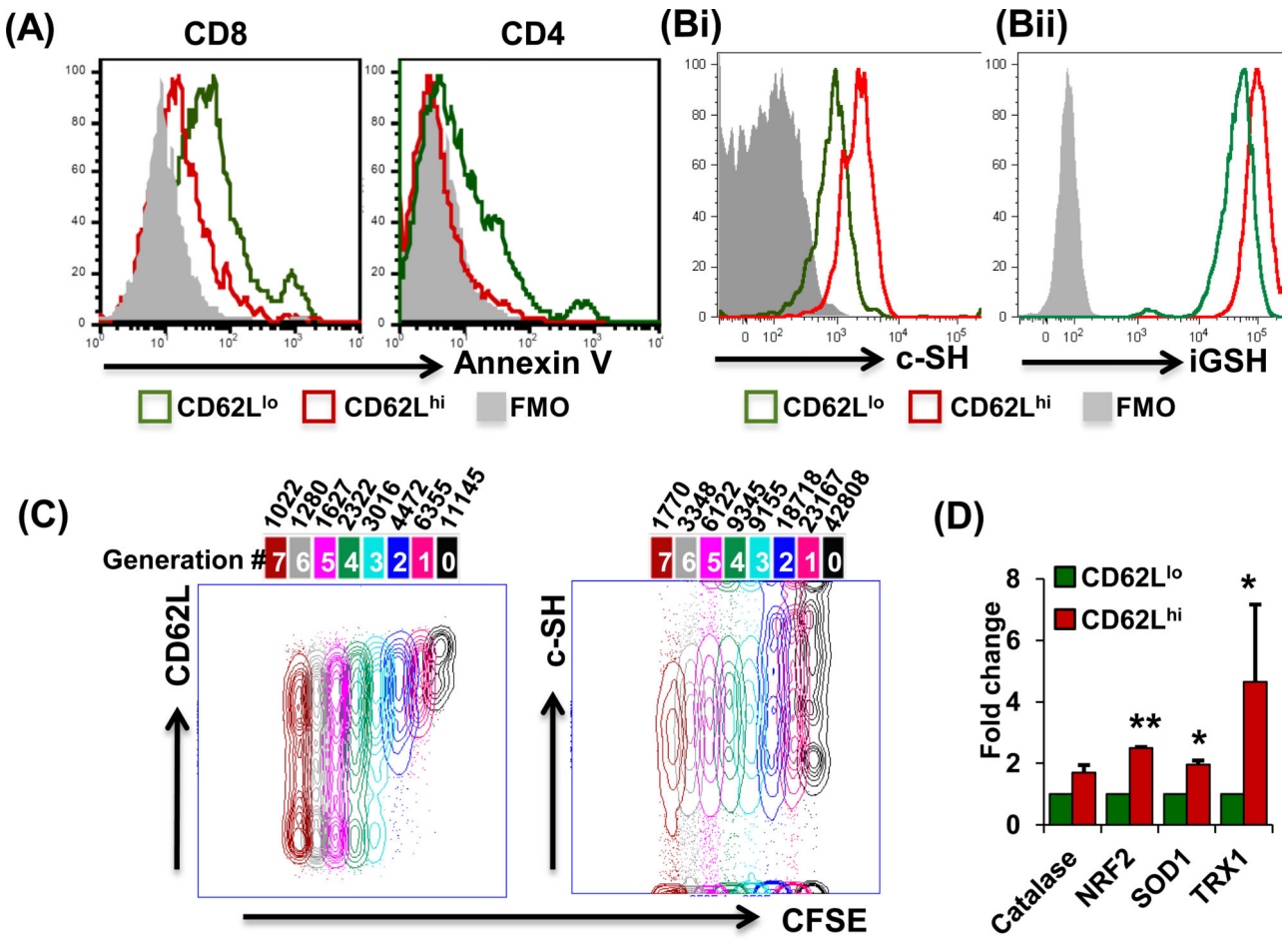

Figure 1. Differential antioxidant capacity in CD62L^{lo} and CD62L^{hi} T cells

(**A**) Activated human PBMCs cultured for seven days were restimulated overnight with anti-CD3 and stained for CD8, CD4, CD62L, and Annexin V for flow-cytometry-based analysis. (**B**) Human T cells were gated on CD8^{+}CD44^{+}CD62L^{hi}CXCR3^{lo}CCR7^{hi} (red) or CD8^{+}CD44^{+}CD62L^{lo}CXCR3^{hi}CCR7^{lo} (green) and analyzed for expression of: (Bi) c-SH using maleamide; $p < 0.05$, and (Bii) iGSH using monochlorobimane; $p < 0.05$. Data are representative of at-least seven experiments with similar results. (**C**) T cells were labeled with CFSE (1 μM) and stimulated or left unstimulated for 72 hours. Cells were then harvested and stained for CD8, Vβ13, CD62L and c-SH, and analyzed by flow cytometry. Cell cycle analysis was then performed using the unstained peak in FlowJo platform software for CD62L and c-SH on CD8^{+} cells. (N = 3) (**D**) PBMCs were cultured in IL-15 for 5 days and sorted as CD8^{+}CD62L^{hi} or CD8^{+}CD62L^{lo} for RNA isolation. mRNA expression levels of antioxidant genes were determined by real-time PCR. All results are representative of three or more separate experiments. ** p <0.005; * p <0.05.

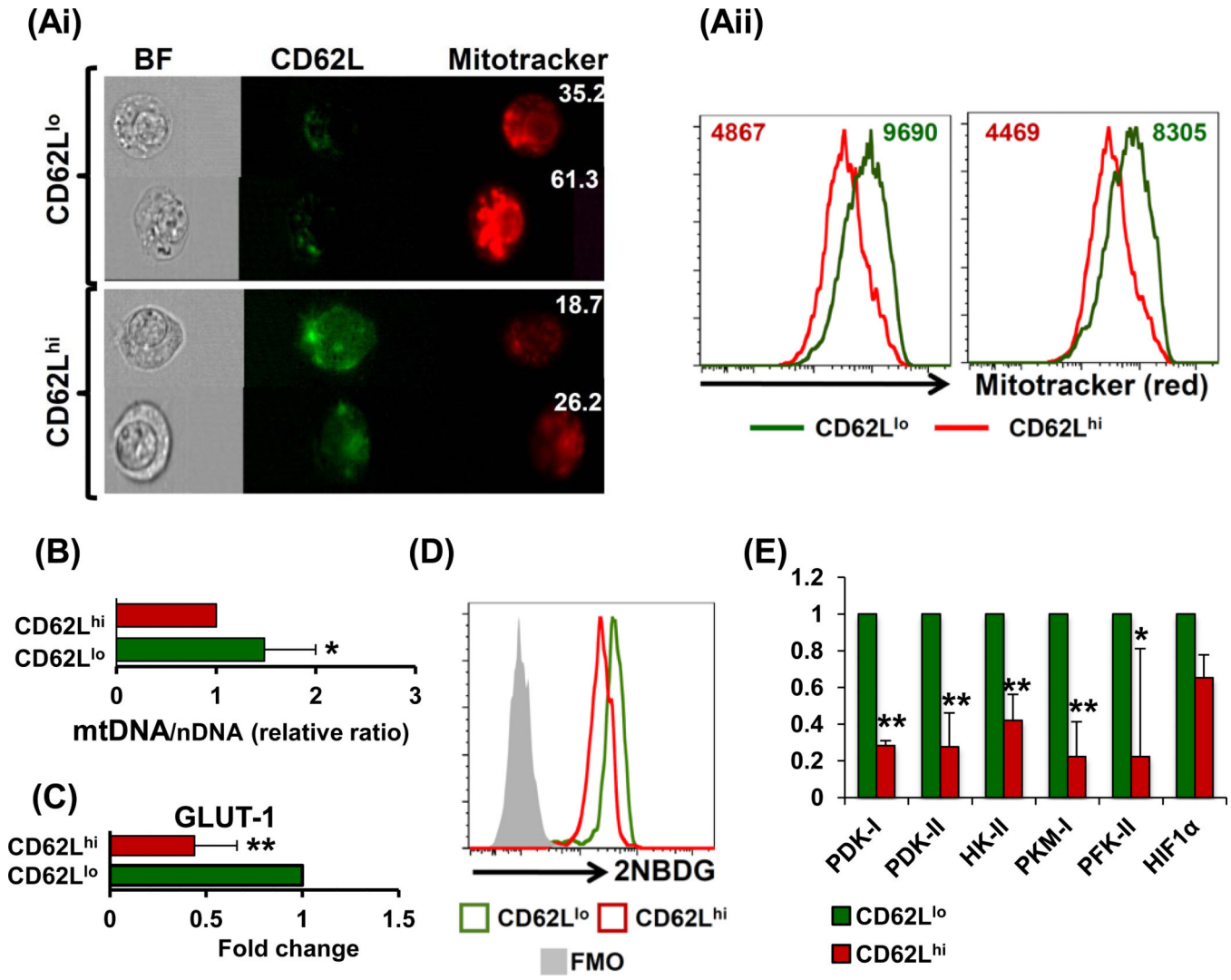

Figure 2. Differences in mitochondrial distribution and glycolysis between CD62L T cell subsets

Human tyrosinase epitope reactive TIL1383I TCR-transduced T cells were cultured in IL-2/IL-15 and used for further experimentation or sorting. (**Ai**) Cells were washed and labeled with fluorochrome-labeled antibodies for CD8, CD34 (TCR), CD62L and Mitotracker red. Cells were acquired on image stream (EMD Millipore Amnis) and analyzed using IDEAS v. 5.0 software. The cells were first gated on $CD8^{+}CD34^{+}$ and then on $CD62L^{lo}$ or $CD62L^{hi}$. The intensity of Mitotracker was compared in these cells. (**Aii**) In a parallel experiment, cells were acquired on BD LSR Fortessa and compared for Mitotracker staining and analyzed using FlowJo software. Experiment was repeated twice with similar results, $p < 0.005$. (**B**) Comparison between the mitochondrial DNA/nuclear DNA ratio (mDNA/nDNA) is shown, $p < 0.05$. (**C**) Real time PCR analysis for GLUT-1 expression between is shown, $p < 0.005$ (N = 3). (**D**) Glucose consumption assay was performed using 2NBGD and its florescence was compared between $CD62L^{lo}$ or $CD62L^{hi}$ cells, $p < 0.005$ (N = 3). (**E**) RNA from sorted as $CD62L^{lo}$ or $CD62L^{hi}$ cells and used to evaluate the differences between glycolysis pathway genes. Results shown were calculated from three separate experiments. ** $p < 0.005$, * $p < 0.05$.

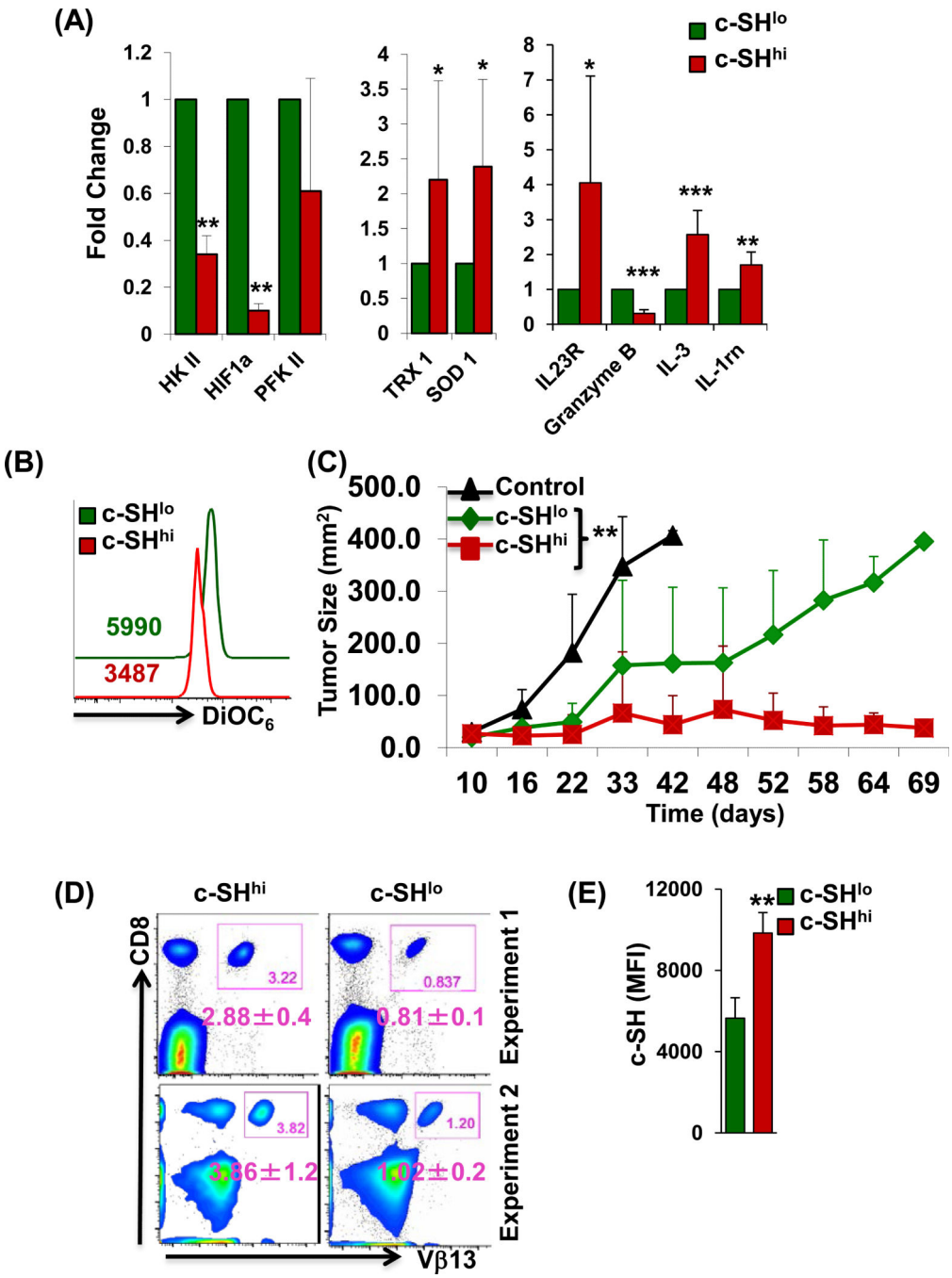

Figure 3. c-SH^{hi} anti-tumor T cells exhibit better tumor control

CD8^{+} transgenic T cells reactive to human gp100 were TCR-activated with cognate antigen along with IL-2 for 3 days. Cells were sorted based on c-SH expression into c-SH^{hi} or c-SH^{lo} fractions. (**A**) mRNA transcripts for key glycolysis genes, antioxidant genes, and effector molecules were analyzed. Data are representative of 3 different samples. * p <0.05, ** p <0.005, *** p <0.0005. (**B**) Membrane potential in c-SH^{hi} or c-SH^{lo} fractions as determined by $DiOC_6$. Numerical values represent MFI, $p < 0.05$ (N = 3). (**C**) Human gp100 reactive CD8^{+} T cells sorted into c-SH^{hi} or c-SH^{lo} fraction were adoptively-transferred to

C57BL/6 mice with subcutaneously established B16-F10 murine melanoma. Tumor growth was monitored as shown. Experiment was repeated twice with 3-5 mice/group/experiment. **p<0.005 Indicates a difference in tumor growth as compared by linear regression model. (**D**) Blood was obtained from each group of mice in **C**, close to the experimental end-point beyond 45 days from two different experiments, and analyzed for the presence of $CD8^+V\beta13^+$ cells. The number in each inset box represents the percentage of $CD8^+V\beta13^+$ cells. The number below each inset box represents the mean±SD percentage of $CD8^+V\beta13^+$ from 3-4 mice of similar groups. (**E**) Cells from blood in **C** were analyzed for c-SH on day 50 post-transfer, and the mean c-SH florescence is shown for mice in each group. Data were analyzed for 3-4 mice per group. ** p <0.005.

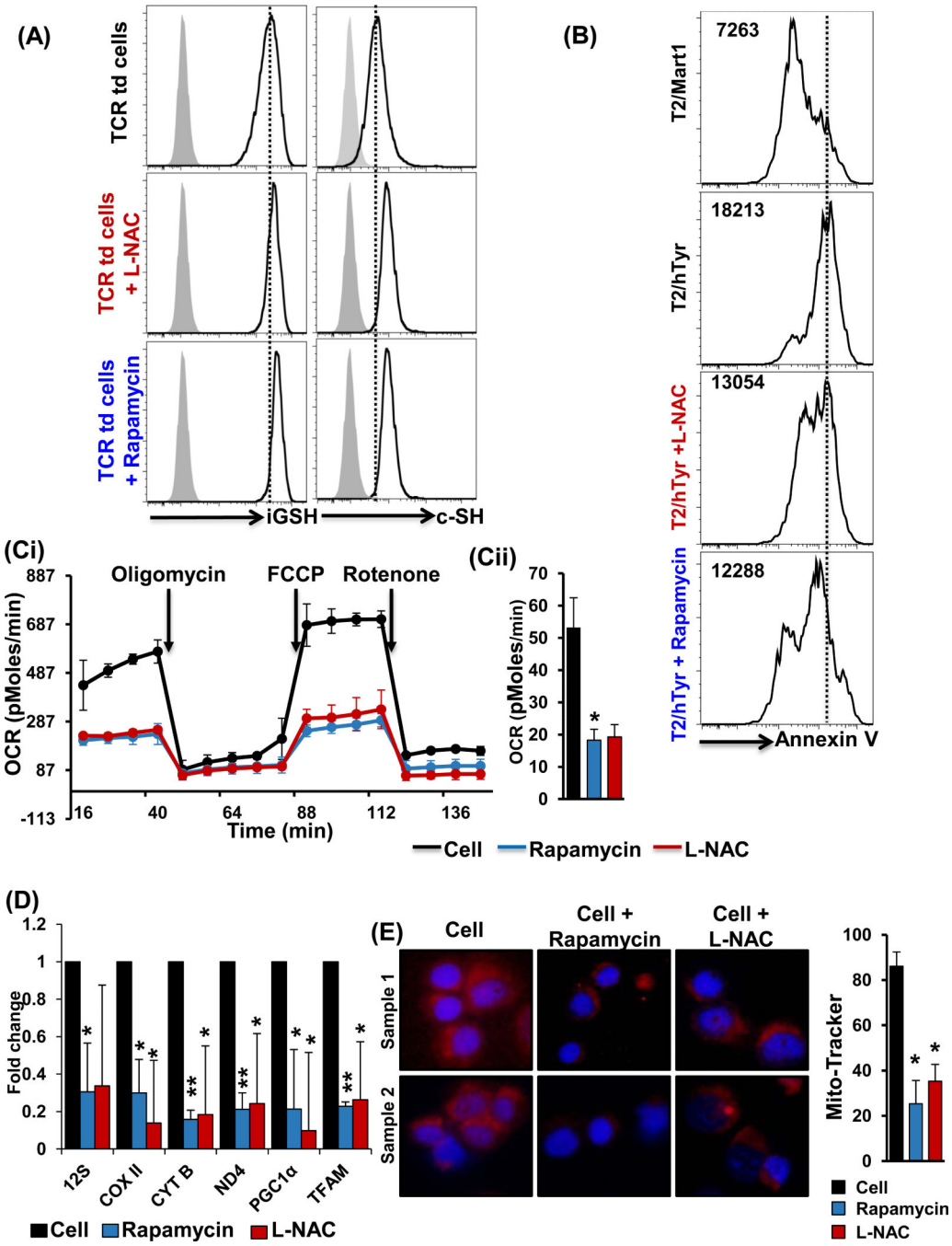

Figure 4. c-SH expression inversely correlates to mitochondrial metabolism in T cells

(**A**) TIL1383I TCR-transduced CD8$^+$ preconditioned cells in rapamycin or L-NAC were analyzed for iGSH ($p < 0.05$; N = 3), and c-SH ($p < 0.05$; N = 3), as described in Methods. (**B**) TIL1383I TCR-transduced CD8$^+$ pretreated with rapamycin or L-NAC was restimulated with either cognate peptide (human Tyrosinase) or control peptide (Mart-1) pulsed T2 cells. Cell death was determined using flow-cytometry-based Annexin V assay. Numbers represent MFI for Annexin V. (**Ci**) Human PBMCs were cultured in IL-15 for 3 days with rapamycin (250 nM), or L-NAC (5 mM) for 30 minutes, or kept untreated. Mitochondrial

respiration was measured by determining oxygen consumption rate using a Seahorse analyzer as detailed in Methods. (**Cii**) Mean from three experiments with similar results is represented. (**D**) TIL1383I TCR-transduced $CD8^+$ T cells preconditioned in rapamycin or L-NAC were analyzed for mitochondrial biogenesis genes and mitochondrial transcription factors using real time PCR analysis. (**E**) Human PBMCs treated with or without rapamycin or L-NAC were stained and analyzed using a fluorescent microscope (60X magnification). Five different fields were photographed for each slide for Mitotracker (red) and DAPI (blue) channels. ImageJ software was used to analyze the difference in Mitotracker intensity. Bar graph on the right represents an average from different experiments. Results are demonstrated as an average of two to three independent experiments with similar results. ** $p < 0.005$, * $p < 0.05$.

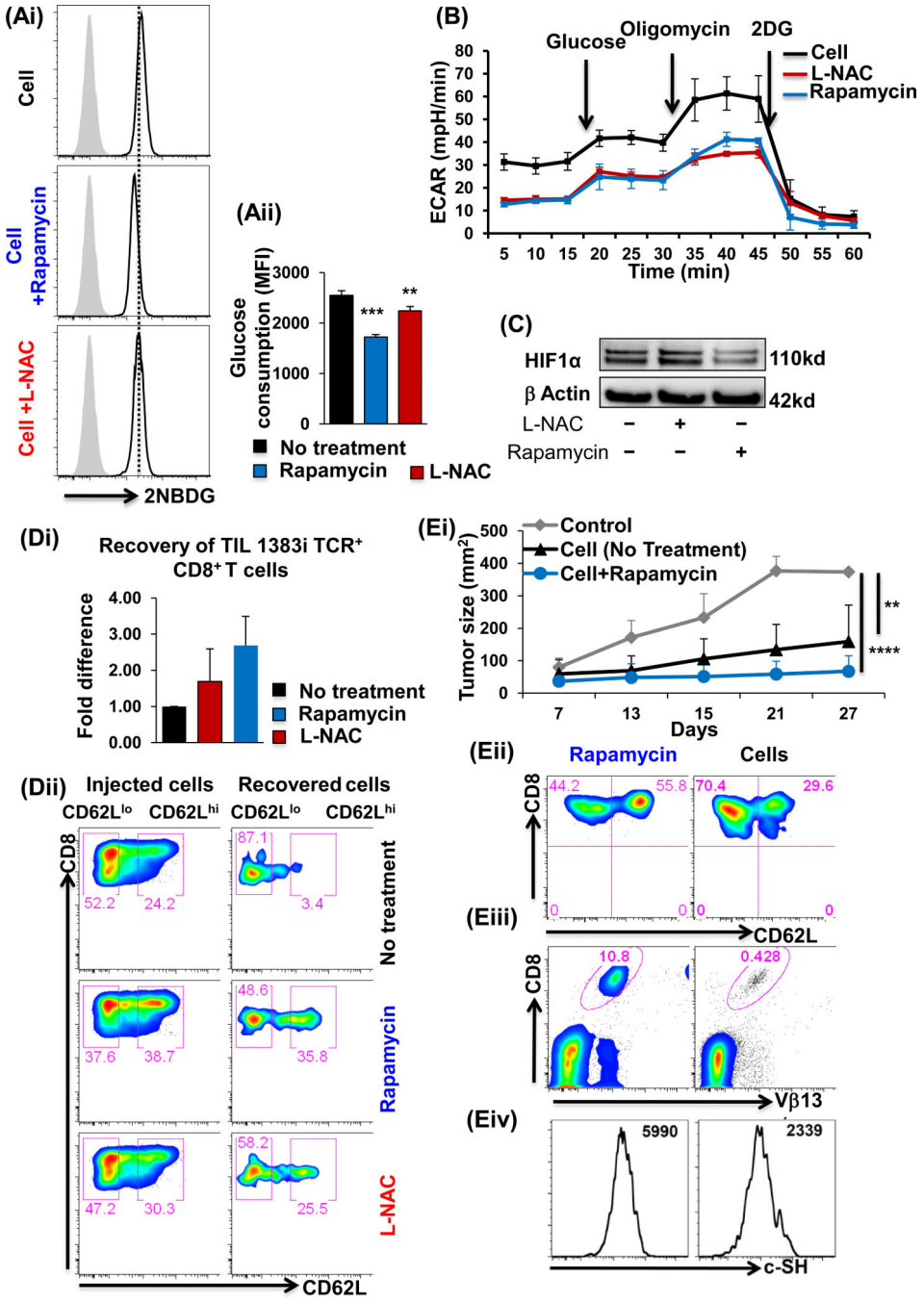

Figure 5. c-SH expression inversely correlates to T cell glycolysis

Human T cells transduced with TIL1383I TCR and cultured in IL-2/IL-15 were treated with/without rapamycin or L-NAC and analyzed for: (**Ai**) Glucose uptake using 2-NBDG on TCR-specific $CD8^+$-gated viable cells as detailed in Methods. (**Aii**) Data represent MFI of 2NBDG from eight different samples. (**B**) ECAR levels using the Seahorse Analyzer, and (**C**) HIF-1α expression by Western blot. (**Di**) Persistence of TIL1383I $CD8^+$ T cells in the spleen of NSG mice 24 h after adoptive transfer. Bar graph represents the number of cells recovered. Experiment was repeated twice. *N=2.* (**Dii**) Comparison of pre- and post-transfer

recovered cells for CD62L expression. Experiment was repeated twice with 3-4 mice/group. **(E)** $CD8^+$ transgenic T cells reactive to human gp100 were activated with cognate antigen in presence/absence of rapamycin along with IL-2 for three days. Equal number of cells were transferred into $Rag^{-/-}$ mice with subcutaneously established murine melanoma B16-F10. Rapamycin group received the maintenance dose of drug (i.p. dose=0.75mg/kg/day from 0-7 days). **(Ei)** Tumor growth was measured twice weekly as shown. Each group had 5 mice, and the experiment was repeated twice. $^{**}p < 0.005$, $^{****}p < 0.00005$. Blood was obtained from each group of mice in **Ei** at the experimental end-point and donor $CD8^+V\beta13^+$ T cells were analyzed for: (**Eii**) CD62L expression, **(Eiii)** Percent of $CD8^+V\beta13^+$ cells ($p < 0.05$), and **(Eiv)** c-SH expression ($p < 0.05$).

Table 1

Effect of Rapamycin on oxidative stress and anti-oxidant defense related genes

Accession No.	Symbol	Description	Fold Change		p value
			Donor 1	Donor 2	
Genes Up- regulated in Rapamycin-treated cells, as compared to untreated control					
NM_001979	EPHX-2	Epoxide hydrolase 2, cytoplasmic	7.78	5.5	0.0385
NM_000581	GPX-1	Glutathione peroxidase 1	3.63	1.82	0.1969
NM_002083	GPX-2	Glutathione peroxidase 2 (gastrointestinal)	1.95	4.79	0.2371
NM_002084	GPX-3	Glutathione peroxidase 3 (plasma)	1.2	1.95	0.2649
NM_002085	GPX-4	Glutathione peroxidase 4 (phospholipid hydroperoxidase)	3.63	2.75	0.0381
NM_015696	GPX-7	Glutathione peroxidase 7	2.75	2.95	0.0029
NM_000637	GSR	Glutathione reductase	3.16	4.47	0.0501
NM_012331	MSRA	Methionine sulfoxide reductase A	3.63	2.39	0.0834
NM_181354	OXR-1	Oxidation resistance 1	2.57	2.75	0.0029
NM_015553	IPCEF-1	Interaction protein for cytohesin exchange factors 1	2.95	2.95	<0.0001
NM_020820	PREX-1	Phosphatidylinositol-3,4,5-trisphosphate-dependent Rac exchange factor 1	2.57	3.16	0.0241
NM_004905	PRDX-6	Peroxiredoxin 6	1.95	2.39	0.0336
NM_005410	SEPP-1	Selenoprotein P, plasma, 1	3.89	33.36	0.3542
NM_003330	TXNRD-1	Thioredoxin reductase 1	2.08	1.58	0.08
NM_006440	TXNRD-2	Thioredoxin reductase 2	1.69	2.75	0.148